Int. J. Electrochem. Sci., 14 **(2019)** 7293 – 7302, doi: 10.20964/2019.08.70

International Journal of
ELECTROCHEMICAL
SCIENCE
www.electrochemsci.org

Short Communication

Constructing Ultrafine Tin Dioxide/Few-Walled Carbon Nanotube Composites for High-performance Supercapacitors

Jianfa Chen[1], *Ting Zhu*[1], *Xiangping Fu*[2], *Guangyuan Ren*[1,*], *Chunyan Wang*[1,*]

[1] Fundamental Science on Radioactive Geology and Exploration Technology Laboratory, Department of Materials Science and Engineering, East China University of Technology, Nanchang, Jiangxi 330013, China
[2] College of Foreign Languages, Jiangxi Agricultural University, Nanchang 330045, China;
[*]E-mail: chywang9902@163.com, gyren@ecit.cn (G. Y. Ren)

Received: 1 May 2018 / *Accepted:* 13 June 2019 / *Published:* 30 June 2019

A hydrothermal/calcination method was successfully applied to prepare ultrafine tin dioxide (SnO_2)/few-walled carbon nanotube (FWNT) composites (SnO_2@FWNT). The corresponding morphological and structural information were further obtained by the characterization technique of transmission electron microscopy, X-ray diffraction, and X-ray photoelectron spectroscopy. In the SnO_2@FWNT composites, ultrafine SnO_2 nanoparticles with an average size of 2–3 nm were uniformly distributed on the FWNT with a thickness of 2–5 layers. With the synergistic effect of highly conductive FWNT and highly dispersed SnO_2, the SnO_2@FWNT hybrids presented excellent specific capacitance of 220.5 F g^{-1} at a scan rate of 2 mV s^{-1} under neutral environment. A power density of 30.63 kW kg^{-1} and an energy density of 512.79 W kg^{-1} were obtained, respectively. In addition, a specific capacity retention rate of 89.57% was acquired after 1000 cycles, indicating a superior stability of SnO_2@FWNT hybrids. The results indicate that the SnO_2@FWNT composites can be used as an alternative electrode material for high-performance supercapacitors.

Keywords: electrode material, supercapacitors, ultrafine tin dioxide, few-walled carbon nanotube
Mobile devices and facilities

1. INTRODUCTION

Supercapacitors (SCs) can deliver higher energy density than conventional dielectric capacitors and higher power density than conventional batteries [1]. So, supercapacitors can be potentially applied in electric automobile, sustaining energy supplies, mobile devices and facilities, and DC power systems [2]. The energy in SCs is usually stored by ion adsorption (electrical double-layer capacitors, EDLCs) or reversible redox reactions (pseudocapacitors) [3]. Electrodes are one of the important components in the supercapacitors, affecting the performance of the whole devices. Therefore, the

reactions occurred at the active materials in the electrodes are closely associated with the energy density and power density of the SCs. At present, the active composition in the electrode of EDLCs are usually carbonaceous materials with abundant intrinsic pores, rapid electron transmission and high specific surface areas, which can adsorb ions rapidly. Hence, EDLCs can deliver much higher power density than conventional batteries. However, the stored energy in EDLCs is limited by the intrinsic ion adsorption capacity of carbon-based materials. To improve the energy density of capacitors, transition-metal oxides or electrically conducting polymers with reversible redox activity are employed as the active materials in the so-called pseudocapacitors [4]. But the power density of pseudocapacitors is lower than EDLCs due to the kinetics of redox reactions is quite low. Therefore, carbon and metal oxides hybrid materials are prepared, which can enhance the redox kinetics, synchronously improving the energy density and power density of the SCs[5] .

Carbon nanotubes (CNTs) have excellent mechanical and electronic properties, showing a great prospect in transistors [6, 7], photovoltaic devices [8, 9], and supercapacitors [10, 11] etc in combination with their unique nanostructures. The CNTs with sidewalls of 2–6 layers or diameters 3 to 8 nm are commonly regarded as few-walled carbon nanotubes (FWNTs). The lengths of FWNTs are in the range of ten or hundred micrometers. In order to apply the FWNTs in supercapacitors, uniform dispersions of FWNTs are needed to obtain evenly electrodes. However, it is difficult to disperse the FWNTs in various solvents due to their inert surface. To improve the dispersion of the FWNTs, their surface is usually modified by functional group. They can still retain the remarkable mechanical and electronic properties due to the unbroken inner layers [12]. So, transition-metal oxides (such as RuO_2, Co_3O_4, and MnO_2) or conducting polymers are incorporated into the FWNTs matrix to further enhance the electrochemical performance of FWNTs [13, 14]. The transition-metal oxides/FWNTs hybrids can serve as suitable electrode materials for supercapacitors, which can deliver excellent rate performance and cyclic stability. Recently, the reported specific capacitance RuO_2/carbon composites can reach up to 570 F/g [15]. However, in consideration of the scarcity of RuO_2, corresponding alternatives like cheap metal oxides (CMOs) are needed to be developed urgently [16–20]. Among the different CMOs, SnO_2 has gained sustained attention due to its excellent chemical stability, low cost, and environmentally friendly features in comparison with RuO_2 [3]. The SnO_2 nanoparticles can be prepared by various methods like arc plasma, sol–gel synthesis, hydrolysis of tin isopropoxide [20], and chemical reduction of stannous chloride followed by calcination [21]. Furthermore, the electrochemical performance of SnO_2 is strongly affected by its corresponding micro-nano structure. So, facile preparation of untrafine SnO_2 nanoparticles with high density of electroactive site is very important for the capacitors.

Herein, we develop a convenient strategy to produce ultrafine SnO_2 nanoparticles, which are supported on FWNTs, forming SnO_2@FWNT composites. A series supercapacitors were fabricated with SnO_2@FWNT composites or FWNTs as the electrode, and each electrochemical performance was evaluated. In result, the hybrid SnO_2@FWNT exhibited good electrochemical performance, which showed great potential in energy devices like supercapacitors.

2. EXPERIMENTAL

2.1. Chemicals and Reagents

FWNTs were purchased from Nanjing XF Nano Technology (China). After an activated approach according to the literature [20], the FWNTs can be used to grow SnO_2 nanoparticles. Other reagents (analytical grade) were bought from Aladdin reagent (China) and were used directly without further purification. The aqueous solutions were prepared with pure water (>18 MΩ).

2.2. Preparation of SnO_2/ FWNT composites

Firstly, to activate FWNTs, they were uniformly dispersed in a nitric acid solution with the assistance of ultrasonic. The resulting dispersion was then heated to 110 ^oC and refluxed for 8 h under a vigorous stirring. After that, the activated FWNTs were subjected to repeated centrifugation and washing with deionized water until the supernatant liquid became neutral. Next, the activated FWNTs were dried at 60 ^oC before use. To prepare the SnO_2/FWNT composites, the 100 mg as-purified FWNTs were dispersed into 100 mL ethylene glycol solution with a round-bottom flask. The mixture was under an ultrasonic treatment till forming a uniform suspension. Then, 1 M NaOH solution was added dropwise into the suspensions until the pH of the dispersions changed to 12. After that, 1 M $SnCl_4 \cdot H_2O$ solution was added into the dispersions under stirring. The resulting homogeneous dispersions were heated to 198 °C and refluxed for 8 h in an oil bath. The products were collected by centrifuging, washing with water several times, and drying under vacuum at 80 °C overnight. Finally, the obtained products were annealed at 500 °C for 2 h, getting the SnO_2@FWNT composites. The preparation process the SnO_2@FWNTs composites is illustrated in Scheme 1.

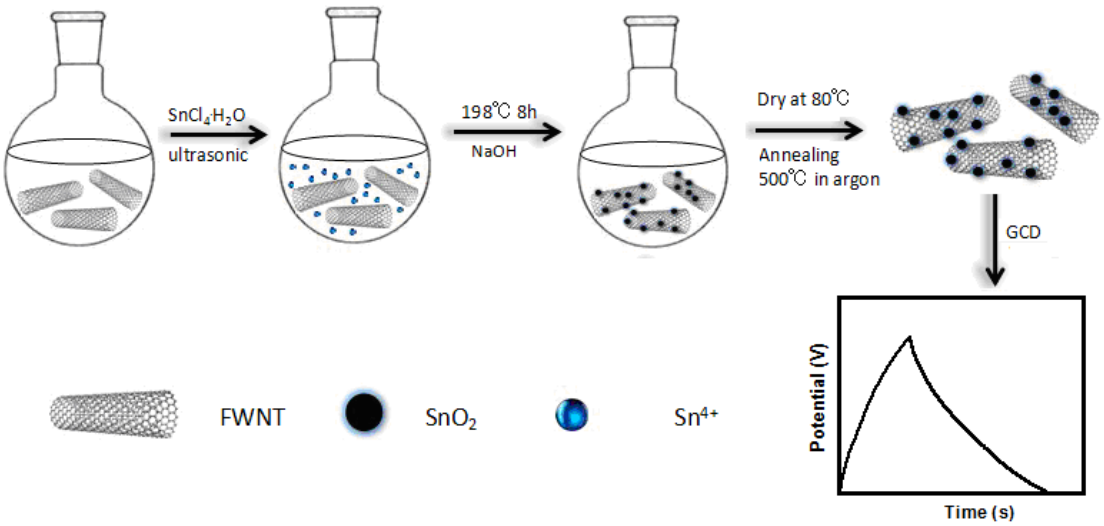

Scheme 1. Illustration of the preparation process of SnO_2@FWNT composites.

2.3. Material Characterization

The morphology of the SnO_2@FWNT composites was characterized by a transmission electron microscope (TEM, Hitachi, JEM-2100) operated at 200 kV. The corresponding structural information was obtained by a powder X-ray diffractometer (XRD, Shimadzu, X-6000, Cu Kα radiation, λ= 0.154 nm) and an X-ray photoelectron spectrometer (XPS, Thermo Fisher, equipped with Al radiation as the probe).

2.4 Preparation of electrode with the SnO_2@FWNT composites

The electrochemical measurements were performed with a CHI 660E electrochemical workstation with a three-electrode system in 1 M Na_2SO_4 solution. The working electrodes were prepared as follows: active materials (SnO_2@FWNT composites), binder (polytetrafluoroethylene) and conductive agent (acetylene black) with a mass ratio of 90:5:5 were dispersed in ethanol, forming a homogeneous slurry under strong stirring. Then, the slurry was coated onto a nickel foam (1 cm × 1 cm) using a doctor blade. After that, the electrode was dried at 80 °C for 12～18 h. A Platinum wire and Ag/AgCl (KCl-saturated) electrode were used as the counter electrode and reference electrode, respectively.

3. RESULTS AND DISCUSSION

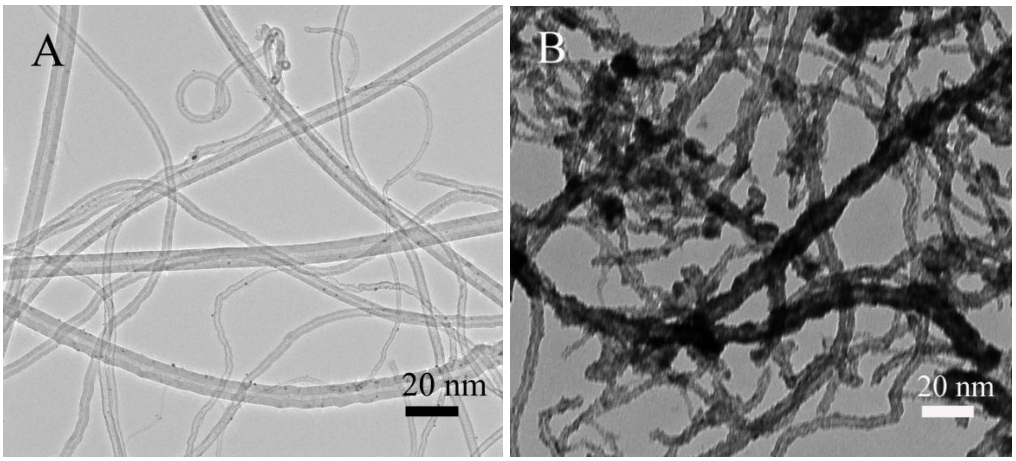

Figure 1. TEM images of (A) FWNTs and (B) SnO_2@FWNT nanocomposites, respectively.

In this work, we developed a facile *in-situ* preparation of FWNTs decorated with ultrafine SnO_2 nanoparticles. The typical procedure is illustrated in Scheme 1. The morphology of as-purified FWNTs is shown in Figure 1A, revealing that the FWNTs like spaghetti, having transparent and one-dimensional (1D) tubular structure. The FWNTs have about 2–5 layers, and the surface of FWNT is clean, indicating that the HNO_3 treatment is very effective for clean-up of the impurities. The TEM image shows that SnO_2 nanoparticles with an average size of 2–3 nm are distributed on the surface of FWNTs as shown in Figure 1B. The SnO_2 particles are ultrafine and SnO_2@FWNT composites still maintain 1D tubular structure, indicating the FWNTs can stabilize the structure of composites. The

formation mechanism of ultrafine SnO_2 particles may be described by the following chemical reactions

$$Sn^{4+} + 4OH^- \longrightarrow Sn(OH)_4$$

$$Sn(OH)_4 \xrightarrow{\text{reflux}} \xrightarrow[500℃]{\text{annealing}} SnO_2$$

The FWNTs and SnO_2@FWNT composites are characterized by powder X-ray diffraction (PXRD), respectively. As shown in Figure 2, the FWNTs show a broad diffraction peak at ~25°, which can be indexed to the characteristic (002) plane of carbon. The broad peaks in SnO_2@FWNTs composites appear at diffraction angles of 27.5°, 34.6°, 52.5°, and 63.5°, corresponding to the (110), (101), (211), and (301) planes of SnO_2, respectively. It indicates that SnO_2 nanoparticles were successfully loaded onto the surface of FWNT and have ultrafine sizes.

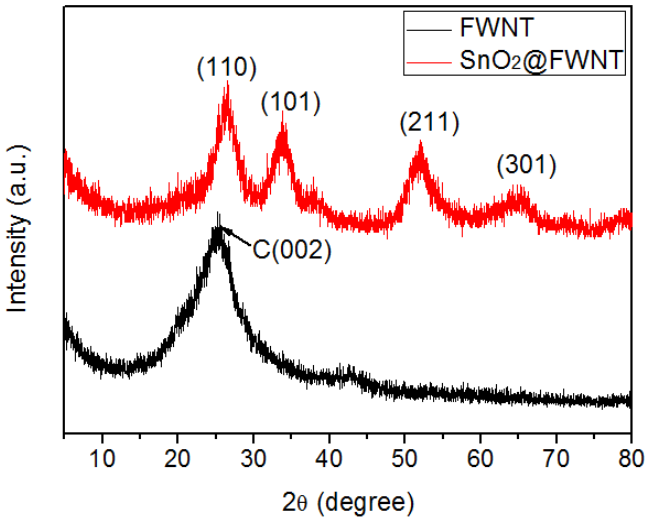

Figure 2. XRD pattern of pure FWNTs and SnO_2@FWNT composites.

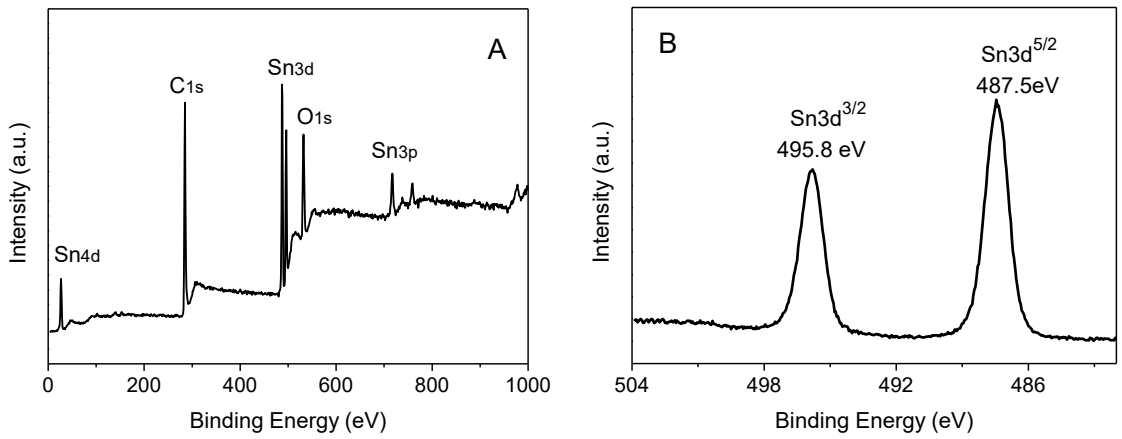

Figure 3. XPS spectra of SnO_2/FWNT composites (A) and (B) high-resolution Sn 3d, respectively.

The XPS spectra can be used to confirm the existence of Sn and corresponding chemical states in the composites. The characteristic peaks of C1s, O1s, Sn4d, Sn3d, and Sn3p can be clearly

identified from the XPS survey spectra as shown in Figure 3A. The high-resolution Sn3d spectra (Figure 3B) shows the peaks of Sn $3d_{3/2}$ (495.8 eV) and Sn $3d_{5/2}$ (487.5 eV). The calculated spin–orbit separation is 8.3 eV, consistent with the reported data of Sn $3d_{3/2}$ and Sn $3d_{5/2}$ in SnO_2 [22]. This indicates that SnO_2/FWNT composites are successfully prepared.

Cyclic voltammetry (CV) is a facile and effective measurement to analyze the capacitive behavior of the nanomaterials. CV measurement of FWNTs or SnO_2/FWNT composites is performed in a 1 M Na_2SO_4 solution at a scan rate of 100 mV/s. The CV of pure FWNT has a rectangular shape, meeting the characteristics of an ideal double-layer capacitor as shown in Figure 4. In addition, the CV curve of SnO_2/FWNT composites has a near-rectangular shape without obvious redox peaks, which indicates that Faraday redox reaction is an electrochemical reversible process [23]. In addition, the SnO_2/FWNT composite shows a higher integrated area than the FWNT electrode, indicating a better capacitance at more negative potential.

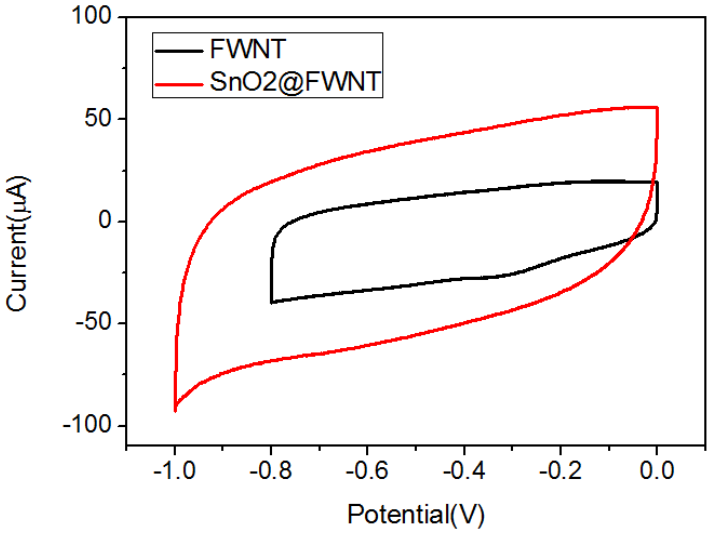

Figure 4. CV curves of FWNTs and SnO_2@FWNT composites at a scan rate of 100 mV/s

Generally, the specific capacitance (Cs) of a material is proportional to the integral area of CV curve. Figure 4 shows that the Cs of SnO_2/FWNT is much larger than FWNT. The electrochemical properties of the capacitor have been significantly improved, which can be attributed to the following structural characteristics. For one thing, the ultrafine SnO_2 nanoparticles can absorb Na^+ on the electrode surface from mild Na_2SO_4 aqueous electrolyte, which are depicted as equation [24]:

$$(O=Sn=O)\ \text{surface} + Na^+ + e \rightarrow (O=Sn=O\ Na^+)\ \text{surface}$$

It is beneficial to provide more sites of the charge storage. For another, SO_4^{2-} is easy to pass through the well-distributed MWCNT network in Na_2SO_4 aqueous solution. As a result, both Na^+ and SO_3^{2-} are fully utilized on the composite electrode.

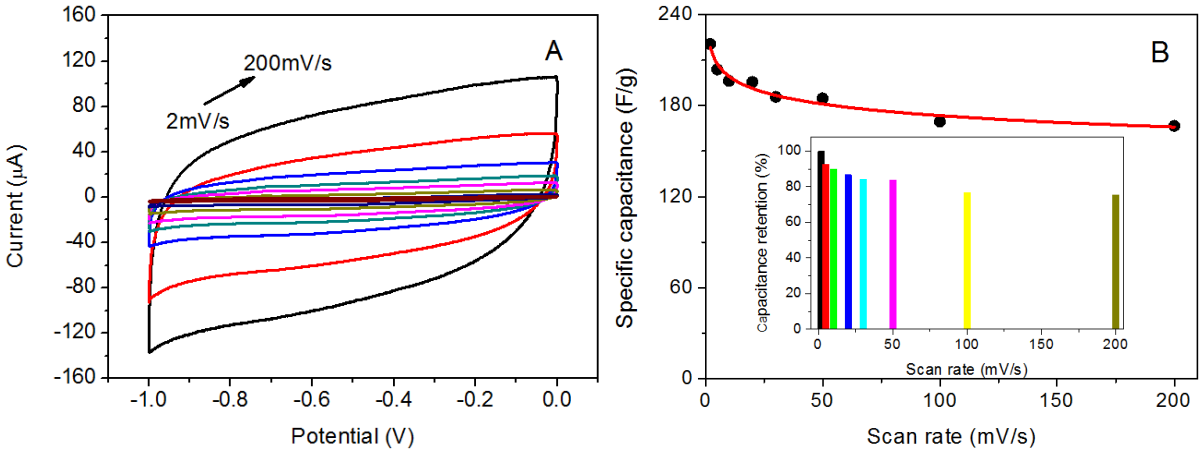

Figure 5. (A) CV curves of SnO_2@FWNT composites scans at various rates from 2 to 200 mV/s. (B) Cs of SnO_2@FWNTs calculated from the CV curves *vs* scan rates. (inset: histogram of Cs retention *vs* scan rates.)

The CV curves of SnO_2/FWNT composites at different scan rates from 2 mV/s to 200 mV/s as shown in Figure 5A. The current gradually improve with the increase of the scan rates. To be noted, all the CV curves present irregular rectangular shapes, especially at high scan rates, indicating pseudocapacitive behaviors in the SnO_2@FWNT composites. It can be ascribed to the intercalation of Na^+ from the electrolyte into the composites and its de-intercalation from the composites to the electrolyte during continuous charging−discharging process. The CV curves of SnO_2/FWNT composites are symmetric, implying a stable structure. It can be attributed to uniform sizes of SnO_2 nanoparticles and the strong anchoring effect of the FWNTs.

The Cs of SnO_2@FWNT composites is calculated from the CV curves with the following equation:

$$C = \frac{1}{mv(V_c - V_a)} \int_{V_a}^{V_c} I(V)dV$$

where I (A) is the response current, v (V/s) is the potential scan rate, $Vc–Va$ (V) is the potential window, and m (g) is the mass of active electrode material. The specific capacitances at the scan rate of 2, 5, 10, 20, 30, 50, 100, and 200 mV/s are 220.5, 203.8, 196.2, 195.5, 185.6, 184.7, 169.3, and 166.5 F/g are, respectively (Figure 5B). The corresponding retention rate at each scan rate is 100%, 92.5%, 90%, 86.6%, 84.2%, 83.8%, 76.8%, and 75.5%, respectively, showing an excellent specific capacitances and power capability. Moreover, the energy density and power density of SnO_2/FWNT composites are 30.63 Wh/kg and 512.79 W/kg, respectively. The results indicate that SnO_2/FWNT composites can be used as an ideal material for the electrode of supercapacitors.

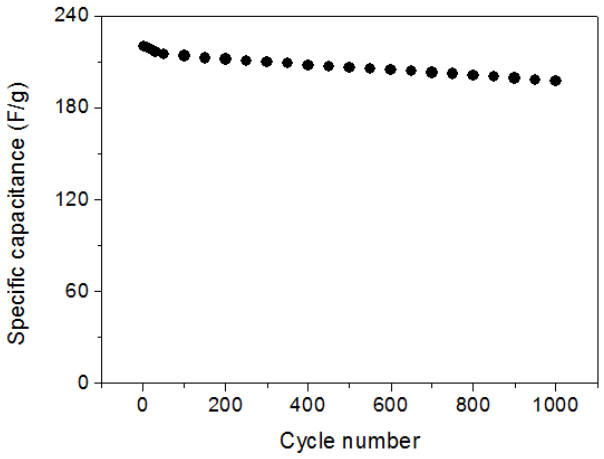

Figure 6. Cycling stability of SnO_2@FWNT composites measured at 2 mV/s

Table 1. Partial list of reported SnO_2-based composites electrode for Cs

SnO_2-based composites	Electrolyte	Cs (F/g)	Reference
SnO_2/MWCNTs	1 M Na_2SO_4	133	[25]
SnO_2/Vulcan carbon	1 M Na_2SO_4	112.14	[25]
SnO_2/CNT	2 M KCl	118.42	[26]
SnO_2/Graphene	1 M H_2SO_4	99.7	[27]
SnO_2/Carbon	1 M KOH	25.8	[28]
SnO_2/Polyaniline	1 M H_2SO_4	305.3	[29]
SnO_2/FWNT	1 M Na_2SO_4	220.5	this work

To evaluate the cycling stability of SnO_2/FWNT composites, a CV test is performed at 2 mV/s for 1000 cycles. As shown in Figure 6, the Cs of SnO_2/FWNT composites decreased from 220.5 F/g to 197.6 F/g after 1000 cycles. The specific capacitance retention rate is 89.57 %, demonstrating a excellent long-term cycling stability. The slight loss of the Cs can be attributed to the dissolution of SnO_2 in the electrolyte during a continuous charge−discharge process.

To demonstrate the superiority of the SnO_2/FWNT composites, a series SnO_2-based composites and corresponding Cs is listed in the Table 1. The SnO_2/FWNT composites in this work have a much higher Cs than the reported references [23-27]. Among these SnO_2-based electrode materials, the good capacitance obtained in this work can be attributed to two aspects: (1) well-dispersed FWNTs not only can provide extra double-layer capacitance, but also can serve as mechanical supporter and conductive network. (2) The *in-situ* growth of SnO_2 can not only prevent the aggregation of FWNTs, but also leads to the formation of uniform and highly-dispersed SnO_2 particles on FWNTs. The excellent electrochemical performances are attributed to synergic effect between ultrafine SnO_2 nanoparticles and highly conductive FWNTs.

4. CONCLUSIONS

We fabricated SnO_2@FWNT composites via a facile hydrothermal and calcination process using FWNT and $SnCl_4 \cdot H_2O$ as the raw materials. The capacitive performance of the SnO_2@FWNT composites was investigated in detail. The composites showed a specific capacitance of 220.5 F/g at a scan rate of 2 mV/s in Na_2SO_4 electrolyte and ~89.57% capacitance retention after 1000 cycles. The power density and energy density were 30.63 kW/kg and 512.79 W/kg, respectively. The results indicate that the SnO_2@FWNT composites have a good potential of in supercapacitors or the other energy devices.

ACKNOWLEDGEMENT
This work is funded by NSF of Jiangxi Province (20171BAB206016), Foundation of Jiangxi Educational Committee (GJJ160536).

References

1. B. E. Conway, Electrochemical supercapacitors: scientific fundamentals and technological applications, *Springer Science & Business Media*, 2013.
2. P. Simon, Y. Gogotsi, *Nat. Mater*., 7 (2008) 845.
3. M. Jayalakshmi, K. Balasubramanian, *Int. J. Electrochem. Sci*., 3 (2008) 1196.
4. Y. Zhang, H. Feng, X. Wu, L. Wang, A. Zhang, T. Xia, H. Dong, X. Li, L. Zhang, *Int. J. Hydrogen Energy*, 34 (2009) 4889.
5. L. L. Zhang, R. Zhou, X. Zhao, *J. Mater. Chem*., 20 (2010) 5983.
6. X. Guo, J. Liu, F. Liu, F. She, Q. Zheng, H. Tang, M. Ma, S. Yao, *Sens. Actuators. B: Chem*., 240 (2017) 1075.
7. X. Li, Y. J. Jeong, J. Jang, S. Lim, S. H. Kim, *Phys. Chem. Chem. Phys.*, 20 (2018) 1210.
8. S. Paul, B. Rajbongshi, B. Bora, R. G. Nair, S. Samdarshi, *New Carbon Materials*, 32 (2017) 27.
9. X. Luo, J. Y. Ahn, Y. S. Park, J. M. Kim, H. W. Lee, S. H. Kim, *Solar Energy*, 150 (2017) 13.
10. L. Li, Z. Lou, W. Han, D. Chen, K. Jiang, G. Shen, *Adv. Mat. Technol*., 2 (2017) 1600282.
11. X. Li, C. Hao, B. Tang, Y. Wang, M. Liu, Y. Wang, Y. Zhu, C. Lu, Z. Tang, *Nanoscale*, 9 (2017) 2178.
12. Y. Hou, J. Tang, H. Zhang, C. Qian, Y. Feng, J. Liu, *ACS Nano*, 3 (2009)1057.
13. Y. Zare, K. Y. Rhee, *RSC. Adv*., 7 (2017) 34912.
14. T. N. Diva, K. Zare, F. Taleshi, M. Yousefi, *J. Nanostruct. Chem.*, 7(2017) 273.
15. Z. S. Wu, D. W. Wang, W. Ren, J. Zhao, G. Zhou, F. Li, H. M. Cheng, *Adv. Funct. Mater*., 20 (2010)3595.
16. L. Bao, T. Li, S. Chen, C. Peng, L. Li, Q. Xu, Y. Chen, E. Ou, W. Xu, *Small*, 13 (2017) 1602077.
17. C. Wang, L. Sun, F. Zhang, X. Wang, Q. Sun, Y. Cheng, L. Wang, *Small*, 13 (2017) 1701246.
18. W. Wei, X. Cui, W. Chen, D. G. Ivey, *Chem. Soc. Rev.*, 40 (2011) 1697.
19. B. Wu, G. Zhang, M. Yan, T. Xiong, P. He, L. He, X. Xu, L. Mai, *Small*, 14 (2018) 1703850.
20. S. de Monredon, A. Cellot, F. Ribot, C. Sanchez, L. Armelao, L. Gueneau, L. Delattre, *J. Mater. Chem*., 12 (2002) 2396.
21. H.-T. Fang, X. Sun, L.-H. Qian, D.-W. Wang, F. Li, Y. Chu, F.-P. Wang, H.-M. Cheng, *J. Phys. Chem. C*, 112 (2008) 5790.
22. M. Chen, H. Wang, L. Li, Z. Zhang, C. Wang, Y. Liu, W. Wang, J. Gao, *ACS Appl. Mater. Interfaces*, 6 (2014) 14327.

23. Y. Qian, C. Huang, R. Chen, S. Dai, C. Wang, *Int. J. Electrochem. Sci.*, 11 (2016) 7453.
24. Y. Liu, Y. Jiao, Z. Zhang, F. Qu, A. Umar, X. Wu, *ACS Appl. Mater. Interfaces* 6 (2014) 2174.
25. V. Vinoth, J.J. Wu, A.M. Asiri, T.L. Villarreal, P. Bonete, S. Anandan, *Ultrasonics Sonochemistry*, 29 (2016) 205.
26. C.H. Xu, J.Z. Chen, *Ceramics International*, 42 (2016) 14287.
27. S. Wang, S.P. Jiang, X. Wang, *Electrochim. Acta*, 56 (2011) 3338.
28. Z. Luo, Y. Zhu, E. Liu, T. Hu, Z. Li, T. Liu, *Mater. Res. Bull*, 60 (2014) 105.
29. Z.A. Hu, Y.L. Xie, Y.X. Wang, L.P. Mo, Y.Y. Yang, Z.Y. Zhang, *Mater. Chem. Phys.*, 114 (2009) 990.

© 2019 The Authors. Published by ESG (www.electrochemsci.org). This article is an open access article distributed under the terms and conditions of the Creative Commons Attribution license (http://creativecommons.org/licenses/by/4.0/).